

- BARTELL, L. S., BROCKWAY, L. O. & SCHWENDEMAN, R. H. (1955). *J. Chem. Phys.* **23**, 1854–1859.
- BASSI, I. W. & SCORDAMAGLIA, R. (1974). *Makromol. Chem.* **175**, 1641–1650.
- BENT, H. (1960a). *J. Chem. Phys.* **32**, 1582–1583.
- BENT, H. (1960b). *J. Chem. Phys.* **33**, 304–305.
- BENT, H. (1960c). *J. Chem. Phys.* **33**, 1259–1260.
- BENT, H. (1960d). *J. Chem. Phys.* **33**, 1260–1261.
- BOWEN, H. J. M., GILCHRIST, A. & SUTTON, L. E. (1955). *Trans. Faraday Soc.* **51**, 1341–1354.
- BURBANK, R. D. (1953). *J. Am. Chem. Soc.* **75**, 1211–1214.
- COSTAIN, C. C. (1958). *J. Chem. Phys.* **29**, 864–874.
- COUTTS, J. W. & LIVINGSTON, R. L. (1953). *J. Am. Chem. Soc.* **75**, 1542–1547.
- CRUICKSHANK, D. W. J. (1965). *Computing Methods in Crystallography*, edited by J. S. ROLLETT, ch. 14. London: Pergamon Press.
- DUNCAN, J. L. (1972). *J. Mol. Struct.* **6**, 447–456.
- ELIEL, E. L., ALLINGER, N. L., ANGYAL, S. J. & MORRISON, G. A. (1965). *Conformational Analysis*, p. 435. New York: Interscience.
- FOURME, R. & RENAUD, M. (1966). *C. R. Acad. Sci. Sér. B*, **263**, 69–72.
- GERMAIN, G., MAIN, P. & WOOLFSON, M. M. (1971). *Acta Cryst.* **A27**, 368–376.
- GHOSH, S. N., TRAMBARULO, R. & GORDY, W. (1952). *J. Chem. Phys.* **20**, 605–607.
- HOLM, R., MITZLAFF, M. & HARTMANN, H. (1968). *Z. Naturforsch. Teil A*, **23**, 307–311.
- HUGHES, D. O. & SMALL, R. W. H. (1972). *Acta Cryst.* **B28**, 2520–2524.
- IMMIRZI, A. (1967). *Ric. Sci.* **37**, 743–749.
- IWASAKI, M. (1959). *Bull. Chem. Soc. Jpn*, **32**, 205–214.
- JEN, M. & LIDE, D. R. (1962). *J. Chem. Phys.* **36**, 2525–2526.
- JOHNSON, C. K. (1970). *ORTEP*. Report ORNL-3794. Oak Ridge National Laboratory, Tennessee.
- KARLE, I. L. & KARLE, J. (1949). *J. Chem. Phys.* **17**, 1052–1058.
- KAWAGUCHI, T., TANAKA, K., TAKEUCHI, T. & WATANABÉ, T. (1973). *Bull. Chem. Soc. Jpn*, **46**, 62–66.
- LIVINGSTON, R. L. & LYON, D. H. (1956). *J. Chem. Phys.* **24**, 1283–1284.
- MILLER, S. L., AAMODT, L. C., DOUSMANIS, G., TOWNES, C. H. & KRAITCHMAN, J. (1952). *J. Chem. Phys.* **20**, 1112–1114.
- MO, F. & SØRUM, H. (1968). *Acta Cryst.* **B24**, 605–615.
- MOORE, F. H. (1963). *Acta Cryst.* **16**, 1169–1175.
- MORINO, Y. & HIROTA, E. (1958). *J. Chem. Phys.* **28**, 185–197.
- MULLER, N. (1953). *J. Am. Chem. Soc.* **75**, 860–863.
- MYERS, R. J. & GWINN, W. D. (1952). *J. Chem. Phys.* **20**, 1420–1427.
- PETERS, D. (1963). *J. Chem. Phys.* **38**, 561–563.
- PICCARDI, P., MODENA, M. & MASSARDO, P. (1973). *Chim. Ind. (Milan)*, **55**, 807.
- SASADA, Y. & ATOJI, M. (1953). *J. Chem. Phys.* **21**, 145–152.
- SCHAEFFER, W. P. & MARSH, R. E. (1969). *Acta Cryst.* **B25**, 1675–1682.
- SCHOMAKER, V. & STEVENSON, D. P. (1941). *J. Am. Chem. Soc.* **63**, 37–40.
- SCHWENDEMAN, R. H. & JACOBS, G. D. (1962). *J. Chem. Phys.* **36**, 1245–1250.
- SILVER, L. & RUDMAN, R. (1972). *J. Chem. Phys.* **57**, 210–216.
- SØRENSEN, A. M. (1971). *Acta Chem. Scand.* **25**, 169–174.
- SUTTON, L. E. (1965). *Tables of Interatomic Distances and Configuration in Molecules and Ions*. Spec. Publ. No. 18. London: The Chemical Society.
- TOWNES, C. H. & SCHAWLOW, A. L. (1955). *Microwave Spectroscopy*. New York: McGraw-Hill.
- VAND, V., EILAND, P. E. & PEPINSKY, R. (1957). *Acta Cryst.* **10**, 303–306.
- WAGNER, R. S. & DAILEY, B. P. (1955). *J. Chem. Phys.* **23**, 1355.
- WAGNER, R. S. & DAILEY, B. P. (1957). *J. Chem. Phys.* **26**, 1588–1593.

*Acta Cryst.* (1979). **B35**, 2650–2655

## Prediction of the Bilayer Packing in the Orthorhombic Phases of Deoxycholic Acid Molecules by van der Waals Energy Calculations

BY S. CANDELORO DE SANCTIS AND E. GIGLIO

*Istituto di Chimica Fisica, Università di Roma, 00185 Roma, Italy*

(Received 23 May 1979; accepted 3 July 1979)

### Abstract

The orthorhombic crystal structures of the deoxycholic acid (DCA) canal complexes so far studied belong to the space group  $P2_12_1$  and are characterized by the association through hydrogen bonds of

the DCA molecules into pleated bilayers. The size and shape of the canals, covered by hydrophobic interior surfaces, and of the guest molecules which can be accommodated depend on the mutual positions along  $b$  and on the separation along  $a$  of two adjacent antiparallel bilayers. The van der Waals energy was com-

0567-7408/79/112650-06\$01.00

© 1979 International Union of Crystallography

puted in the crystals, neglecting the guest molecules, by moving the bilayers along **b** for different values of **a**. The observed host lattices fit the minima of the van der Waals energy. The analysis of the energy results allowed an approximate prediction to be made for the orthorhombic choleic acid crystals of the shape and size of the molecules which may be occluded and the packing of the bilayers, once the cell dimensions were known.

### Introduction

3 $\alpha$ ,12 $\alpha$ -Dihydroxy-5 $\beta$ -cholan-24-oic acid (deoxycholic acid, DCA, Fig. 1) forms canal complexes, termed choleic acids, with many molecules (Sobotka, 1934; Fieser & Fieser, 1959; Herndon, 1967). The DCA molecule has one hydrophobic and one hydrophilic side and a remarkable ability to associate by means of stable hydrogen-bonding schemes in the solid state. To our knowledge DCA crystallizes in orthorhombic, hexagonal and tetragonal phases giving rise to inclusion compounds. So far some crystal structures of orthorhombic canal complexes, all belonging to the space group  $P2_12_12_1$ , have been solved (see Table 1 for abbreviations, cell parameters and stoichiometry), the acholic constituents being acetic acid (Craven & DeTitta, 1972), acetophenone, acetone and diethyl ketone (Lahav, Popovitz-Biro, Tang & Leiserowitz, 1977; Lahav, Leiserowitz, Popovitz-Biro & Tang, 1978; Tang, 1978), *p*-diiodobenzene and phenanthrene (Candeloro De Sanctis, Giglio, Pavel & Quagliata, 1972), (*R*)-3-methylcyclohexanone and cyclohexanone (Tang, 1978), norbornadiene (Fedeli, Giglio, Mazza & Pavel, unpublished data) and di-*tert*-butyl diperoxycarbonate (Friedman, Lahav, Leiserowitz, Popovitz-Biro, Tang & Zaretskii, 1975). Moreover, two hexagonal canal complexes, space group  $P6_s$ , formed by DCA, ethanol and water in the ratio 3:2:1 (Candeloro De Sanctis, Coiro, Giglio, Pagliuca, Pavel & Quagliata, 1978) and by DCA, dimethyl sulphoxide and water in the ratio 2:1:1 (Candeloro De Sanctis, Giglio, Petri & Quagliata, 1979), together with two tetragonal phases, space group  $P4_12_12$ , composed of DCA and water in the ratio 2:3 (Lahav, Leiserowitz & Tang, private communication) and by DCA, ethanol and water in the ratio 2:1:1 (Coiro, D'Andrea & Giglio, 1979) have been investigated. The guest molecules are accommodated in canals with interior surfaces which are mainly hydrophobic in the orthorhombic or hydrophilic in the hexagonal and tetragonal crystals. Thus hydrophobic interactions or hydrogen bonds are the chief forces which hold together host and guest molecules.

The aim of this work is a study of the packing in the orthorhombic phases, characterized by pleated bilayers parallel to  $bc$  in which the DCA molecules are

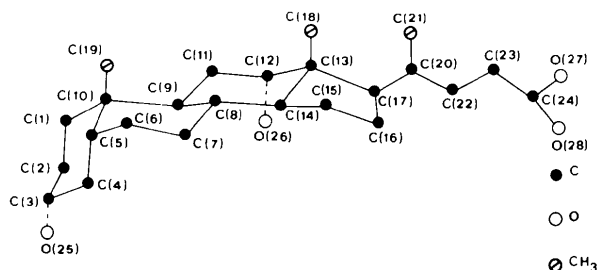


Fig. 1. The DCA molecule and its atomic numbering.

Table 1. Cell parameters (Å) and compositions of some orthorhombic choleic acids

Abbreviation	Guest	DCA/ guest	<i>a</i>	<i>b</i>	<i>c</i>
DCAACA	Acetic acid	1:1	25.55	13.81	7.11
DCAAPH	Acetophenone	2.5:1	25.59	13.71	7.25
DCAACE	Acetone	2:1	25.81	13.61	7.23
DCADEK	Diethyl ketone	2:1	25.83	13.56	7.24
DCAPIB	<i>p</i> -Diiodobenzene	2:1	26.59	13.58	7.17
DCAPHE	Phenanthrene	3:1	26.81	13.60	21.66*
DCAMCH	3-Methylcyclohexanone	2:1	26.96	13.52	14.16
DCACHX	Cyclohexanone	2:1	26.99	13.35	14.16
DCANBD	Norbornadiene	2:1	27.13	13.46	14.21
DCADTB	Di- <i>tert</i> -butyl diperoxycarbonate	4:1	27.16	13.48	14.17

\* The translation period of DCA along *c* is 7.22 Å.

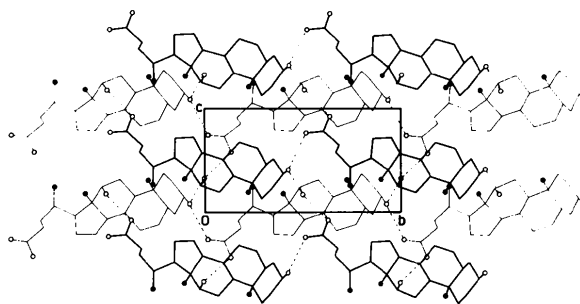


Fig. 2. Molecular packing of a DCAACA bilayer viewed along **a**. Black and open circles represent methyl groups and O atoms respectively. The dashed lines indicate hydrogen bonding.

associated through an efficient system of hydrogen bonds formed by hydroxyl and carboxyl groups (Fig. 2). Two adjacent bilayers are antiparallel and give rise to canals, running along **c**, with dimensions and shape depending on **a** and on the bilayer position along **b**. Figs. 3 and 4 show two different cavities, adapted to the size of the guest molecule, for the DCAACA and DCAPHE crystals.

Table 1 suggests the occurrence of two groups of choleic acids, hereafter indicated  $\alpha$  and  $\beta$ , with the

translation period of DCA along  $c$  of  $\sim 7.2$  and  $\sim 14.2$  Å respectively, and with nearly equal bilayers (Figs. 2 and 5). A bilayer is composed of two wavy monolayers, each formed by rows of DCA molecules linked in each row by head-to-tail hydrogen bonds involving O(25) and O(27) of two consecutive molecules. In the  $\beta$  group there are intermediate rows, almost halfway between the two rows at, for example,  $c \simeq 0$  and  $c \simeq 14.2$  Å (Fig. 5), which cannot be reproduced by an exact translation of  $\sim 7.2$  Å along  $c$  as occurs in the  $\alpha$  group. Furthermore, the rows of two-faced monolayers, belonging to two adjacent bilayers, are shifted in the  $bc$  projection by  $\sim 3.6$  Å along  $c$  in the  $\alpha$  group, while they are at nearly the same height on  $c$  in the  $\beta$  group.

Moreover, the values of the cell constants of Table 1 show the trend of  $a$  to increase from 25.6 to 27.2 Å with the bulkiness of the occluded molecule, without limit in the direction parallel to  $c$ . The parameters  $b$  and  $c$  undergo small changes for the  $\alpha$  group within the ranges 13.6–13.8 Å and 7.1–7.3 Å and for the  $\beta$  group the ranges are even narrower so that  $b$  varies

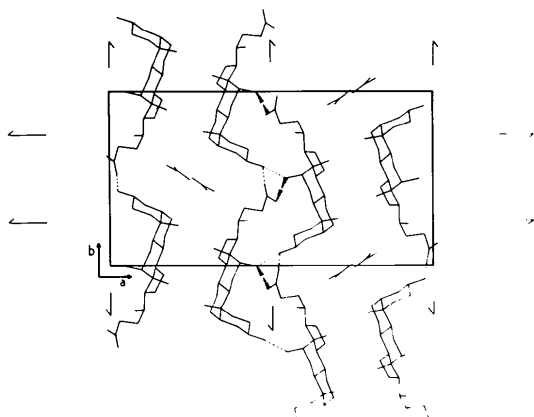


Fig. 3. DCAACA crystal packing viewed along  $c$ . The dashed lines represent hydrogen bonding.

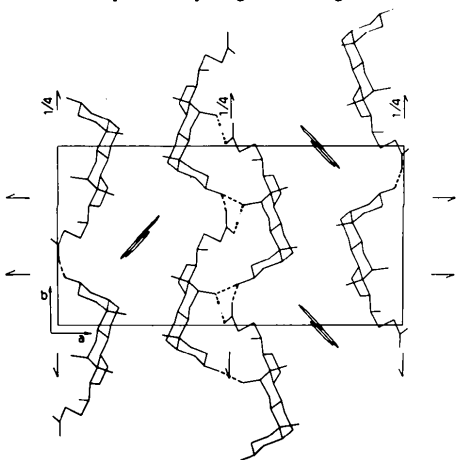


Fig. 4. DCAPHE crystal packing viewed along  $c$ . The dashed lines represent hydrogen bonding.

from 13.4 to 13.5 Å and  $c$  can be considered constant (14.2 Å). Thus, since  $a$  is influenced by the bilayer separation and the other two parameters are connected with the bilayer structure, this can reasonably be assumed to be practically equal in each  $\alpha$  or  $\beta$  group. The experimental data so far acquired support this assumption and show that the DCA geometry and conformation remain approximately unchanged.

On the basis of these considerations we attempted to establish if it were possible to foresee *a priori* the bilayer packing as a function of  $a$  and of the bilayer translation along  $b$  by means of van der Waals energy calculations, neglecting the contribution of the acholic constituent.

#### Van der Waals energy calculations

Energy calculations were performed for the groups  $\alpha$  and  $\beta$  in the space group  $P2_12_12_1$  with the  $b$  and  $c$  parameters as well as the final atomic coordinates (Table 2) of DCAACE and DCANBD respectively. The H atoms, except those of the hydroxyl, carboxyl and methyl groups, were generated by putting  $C-H = 1.08$  Å and  $H-C-C = 109.5^\circ$ . The H atoms bonded to the tertiary C atoms make two  $H-C-C$  bond angles of  $109.5^\circ$ , the third being determined by the non-regular tetrahedral hybridization of the above-mentioned C atoms. The methyl group was treated as one atom.

The coefficients of the potentials expressed as  $V(r) = a \exp(-br)/r^d - cr^{-6}$ , and used to describe van der Waals interactions among non-bonded atoms, are reported in Table 3 (Pavel, Quagliata & Scarcelli, 1976, and references therein).

The interactions between the DCA asymmetric unit and the sixteen nearest DCA molecules, belonging to four rows of the same monolayer different from that of the DCA asymmetric unit, were considered in the calculations by assuming a cut-off distance of 7.5 Å. These two monolayers are faced and separated by canals.

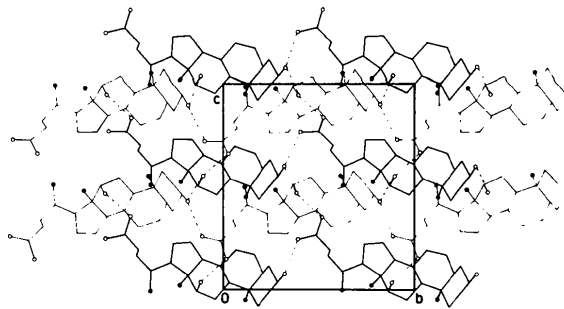


Fig. 5. Molecular packing of a DCANBD bilayer viewed along  $a$ . Black and open circles represent methyl groups and O atoms respectively. The dashed lines indicate hydrogen bonding.

Table 2. Fractional atomic coordinates ( $\times 10^3$ ) of DCA in the DCAACE and DCANBD crystal structures

	DCAACE			DCANBD, 1st molecule			DCANBD, 2nd molecule		
	x	y	z	x	y	z	x	y	z
C(1)	119	273	150	110	181	-79	119	189	432
C(2)	65	299	208	60	215	-45	70	219	476
C(3)	68	373	365	66	287	35	79	290	554
C(4)	98	329	523	95	242	116	112	245	631
C(5)	153	297	466	147	208	81	161	212	586
C(6)	184	253	636	177	165	164	195	169	665
C(7)	164	155	690	157	63	195	179	67	697
C(8)	163	81	525	151	-11	114	169	-5	616
C(9)	131	125	366	120	33	34	134	39	543
C(10)	153	226	297	143	134	-3	153	140	503
C(11)	123	49	211	109	-41	-45	121	-36	465
C(12)	100	-48	280	86	-139	-7	98	-132	506
C(13)	133	-93	432	119	-185	70	133	-179	580
C(14)	136	-15	588	127	-107	148	145	-101	654
C(15)	162	-74	750	151	-166	229	172	-160	731
C(16)	137	-175	736	125	-264	225	143	-259	732
C(17)	107	-178	550	96	-271	131	111	-264	643
C(18)	186	-127	357	168	-221	23	180	-217	525
C(19)	207	214	220	194	117	-46	205	124	452
C(20)	108	-285	469	95	-377	90	107	-371	602
C(21)	82	-293	279	68	-384	-2	78	-377	510
C(22)	86	-360	611	78	-454	164	87	-443	678
C(23)	32	-342	661	25	-438	194	34	-425	706
C(24)	12	-423	791	9	-515	267	14	-502	771
O(25)	17	396	418	17	315	69	30	315	597
O(26)	48	-32	337	37	-121	29	50	-109	548
O(27)	11	-510	749	9	-606	246	29	-590	772
O(28)	-7	-395	947	-6	-486	348	-20	-476	829

Table 3. The coefficients of the semi-empirical potential functions

The energy is in  $\text{kJ}/4 \cdot 18$  per atom pair if the interatomic distance is in  $\text{\AA}$ .

Interaction	$a \times 10^{-3}$	$b$	$c$	$d$
H-H	6.6	4.080	49.2	0
H-C	44.8	2.040	125.0	6
H-O	42.0	2.040	132.7	6
H-CH <sub>3</sub>	49.1	3.705	380.5	0
C-C	301.2	0	327.2	12
C-O	278.7	0	342.3	12
C-CH <sub>3</sub>	291.1	1.665	981.1	6
O-O	259.0	0	358.0	12
O-CH <sub>3</sub>	272.7	1.665	1026.3	6
CH <sub>3</sub> -CH <sub>3</sub>	273.9	3.329	2942.0	0

The van der Waals energy curves computed for DCAACE and DCANBD as a function of  $y$  at different values of  $a$  are reported in Figs. 6 and 7. The  $y$  values represent the increments given to the  $y$  atomic coordinates of Table 2, corresponding to  $y = 0 \text{ \AA}$ .

The parameters  $a$  and  $y$  were varied with increments of  $0.2$  and  $0.1 \text{ \AA}$  respectively.

### Discussion

The deepest minimum zone in Fig. 6 for  $25.2 \leq a \leq 26.0 \text{ \AA}$  is located within the range  $0.0 \leq y \leq 0.5 \text{ \AA}$  and

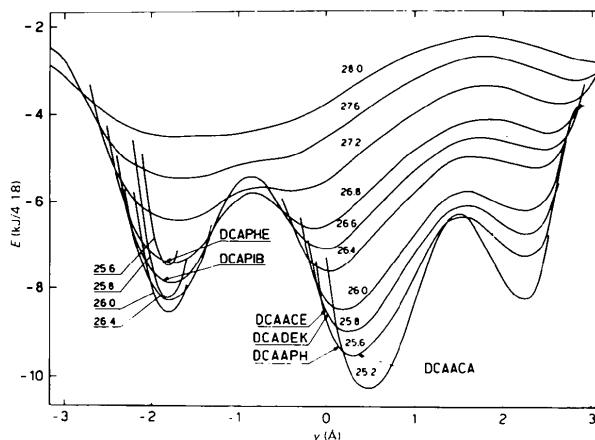


Fig. 6. Van der Waals energy vs  $y$  for different values of  $a$  for DCAACE. The arrows indicate the positions of the experimental crystal structures.

is populated by the DCAACA, DCAAPH, DCAACE and DCADEK observed crystal structures of the  $a$  group (see Fig. 3 as an example). The lowest minimum is shifted in the range  $-1.9 \leq y \leq -1.7 \text{ \AA}$  for  $a > 26.0 \text{ \AA}$ , where the bilayer packing of DCAPIB and DCAPIB is found (Fig. 4). This decreasing of  $y$  and the increasing of  $a$  passing from DCAACA to DCAPIB cause a change in both the dimensions and shapes of the sections of the canals perpendicular to  $c$ .

The sizes of the canals in the  $ab$  plane rise from  $\sim 2.8 \times 5.5$  Å to  $\sim 4.1 \times 7.3$  Å, allowing the accommodation of bulkier molecules. The relative shape remains rectangular in both cases. However, the long side of the rectangle in DCAACA is rotated about  $80^\circ$  around the  $c$  axis in comparison with that of DCAPHE, so that the acetic acid and phenanthrene molecular planes form an angle of about  $80^\circ$ .

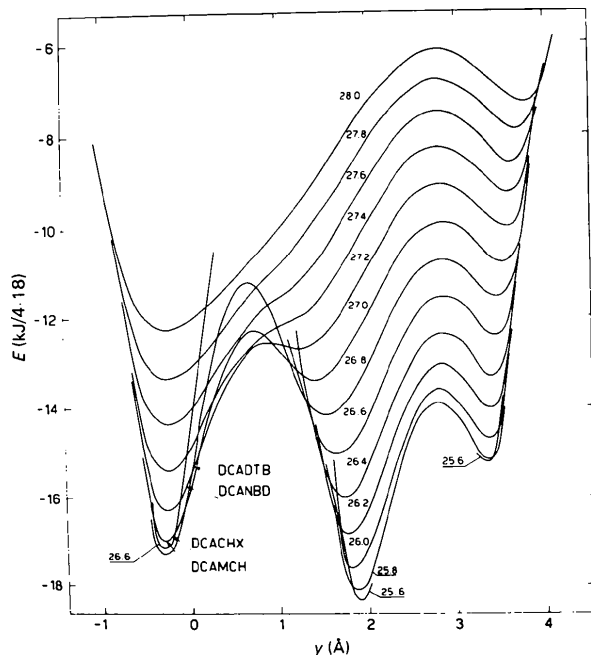


Fig. 7. Van der Waals energy  $vs$   $\gamma$  for different values of  $a$  for DCANBD. The arrows indicate the positions of the experimental crystal structures.

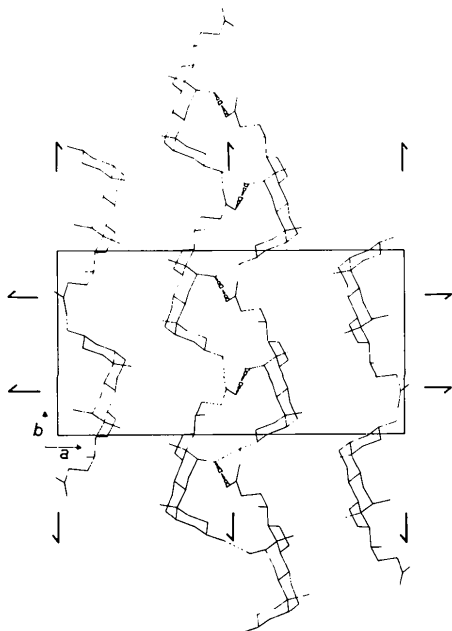


Fig. 8. DCA packing, corresponding to  $a = 25.6$  Å and  $\gamma = 2.25$  Å, viewed along  $c$  for the  $\alpha$  group.

Another minimum region, always higher than at least one of the two previously mentioned, occurs at  $\gamma \approx 2.25$  Å and corresponds to the packing seen in Fig. 8, never observed so far. Fig. 8 shows the disappearance of the cavities in the structure, which, therefore, cannot include guest molecules. These three minima zones, in order, will be indicated as  $A$ ,  $B$  and  $C$ .

The minimum-point energy values of the curves of Fig. 6 in the regions of the DCAACA, DCAPHE and 'without-canals' structures are reported  $vs$   $a$  in Fig. 9. The curves  $A$ ,  $B$  and  $C$  refer to the corresponding minima zones. Curves  $A$  and  $B$  cross each other at  $a \approx 26.0$  Å and present the minimum value of the energy at  $24.9$  and  $26.1$  Å, whereas curve  $C$  is always increasing and above one, at least, of the other two curves. Thus, guest molecules of small size or which are thread-like can be accommodated in the canals of DCAACA type, whereas aromatic molecules containing, for example, one benzene ring and bulky substituents such as iodine or two or more benzene rings can be occluded in those of the DCAPHE type. Preliminary results on DCA adducts of palmitic acid, naphthalene, and 1,2-benzanthracene seem to support this statement.

The  $\beta$  structures also present three minimum regions, indicated as  $A'$ ,  $B'$  and  $C'$ , corresponding to minima centred at about  $1.75$ ,  $-0.25$  and  $3.40$  Å of  $\gamma$  (Fig. 7) and nearly comparable with  $A$ ,  $B$  and  $C$  respectively for the bilayer position along  $b$ . However, the crystal structures so far known show that only the region  $B'$  is populated when  $a \geq 27.0$  Å and the guest molecules are or have groups of approximate spherical shape. Their bulkiness causes the increasing of  $a$  and makes the cavities of the choleic acid crystals closer to squares.

The minimum-point energy values in the regions  $A'$ ,  $B'$  and  $C'$  are reported  $vs$   $a$  in Fig. 10. The 'without-canals' packing of  $C'$  gives rise to energy values higher than those of one, at least, of the other two structures,  $A'$  and  $B'$ . The minima of  $A'$  and  $B'$  are centred at  $a$  equal to  $25.6$  and  $26.8$  Å,  $B'$  being more stable than  $A'$  from  $26.6$  Å upward.

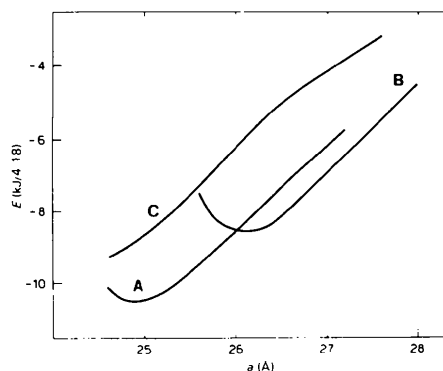


Fig. 9. Curves of the lowest energy values for the  $A$ ,  $B$  and  $C$  minimum regions as a function of  $a$ .

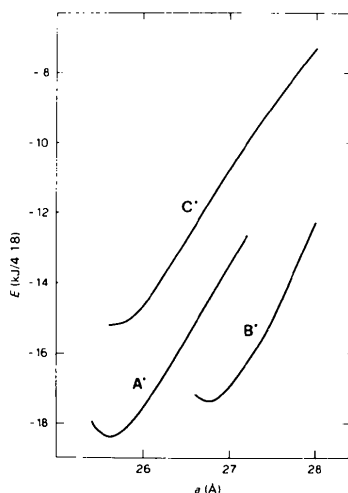


Fig. 10. Curves of the lowest energy values for the  $A'$ ,  $B'$  and  $C'$  minimum regions as a function of  $a$ .

Since the DCANBD and DCAACE asymmetric units are formed by two and one DCA molecules respectively, the energy values of Fig. 10 must be halved when compared with those of Fig. 9. Thus  $A$  is energetically favoured with respect to  $A'$  and this may explain why the  $A'$  region is not populated. On the other hand, since for  $a \geq 26.6 \text{ \AA}$   $B'$  is more stable than  $B$ , the  $\beta$  structures may be preferred when a large  $a$  is required owing to the size of the guest molecules.

Moreover, the DCA molecules seem to be slightly more closely packed in the  $\beta$  rather than in the  $\alpha$  bilayer on the basis of the  $b$  and  $c$  parameters (Table 1) and of the bilayer thickness on  $a$ , measured for DCANBD and DCAACE.

Miyata & Takemoto (1978) in the course of research on inclusion polymerizations have found that some guest molecules, such as acetic acid and acetone, can be released from their orthorhombic DCA canal complexes and replaced by 2,3-dimethyl-1,3-butadiene (DMB), which fits into the DCA canals, by heating DCAACA or DCAACE with an excess of DMB in a sealed tube for 1 h at 333 K.

By studying the replacement of the guest molecules by DMB as a function of temperature and time Miyata

& Takemoto observed that replacement of acetone by the larger DMB molecule was much easier than the replacement of acetic acid. Thus, if the host-guest interactions are nearly equal, these findings can be accounted for on the assumption that the more similar the dimensions of the canals corresponding to the guest molecules which replace each other, the more easily the replacement occurs. In fact, it is reasonable to suppose that the adduct of DCA with DMB should have  $y$  negative in Fig. 6, so that it has canals which are more similar to those of DCAACE than to those of DCAACA.

The authors thank the Consiglio Nazionale delle Ricerche for financial support.

#### References

- CANDELORO DE SANCTIS, S., COIRO, V. M., GIGLIO, E., PAGLIUCA, S., PAVEL, N. V. & QUAGLIATA, C. (1978). *Acta Cryst.* **B34**, 1928–1933.
- CANDELORO DE SANCTIS, S., GIGLIO, E., PAVEL, V. & QUAGLIATA, C. (1972). *Acta Cryst.* **B28**, 3656–3661.
- CANDELORO DE SANCTIS, S., GIGLIO, E., PETRI, F. & QUAGLIATA, C. (1979). *Acta Cryst.* **B35**, 226–228.
- COIRO, V. M., D'ANDREA, A. & GIGLIO, E. (1979). *Acta Cryst.* **B35**. In the press.
- CRAVEN, B. M. & DETITTA, G. T. (1972). *Chem. Commun.* pp. 530–531.
- FIESER, L. F. & FIESER, M. (1959). *Steroids*, ch. 3, pp. 115–118. New York: Reinhold.
- FRIEDMAN, N., LAHAV, M., LEISEROWITZ, L., POPOVITZ-BIRO, R., TANG, C. P. & ZARETZKII, Z. (1975). *Chem. Commun.* pp. 864–865.
- HERNDON, W. C. (1967). *J. Chem. Educ.* **44**, 724–728.
- LAHAV, M., LEISEROWITZ, L., POPOVITZ-BIRO, R. & TANG, C. P. (1978). *J. Am. Chem. Soc.* **100**, 2542–2544.
- LAHAV, M., POPOVITZ-BIRO, R., TANG, C. P. & LEISEROWITZ, L. (1977). Fourth European Crystallographic Meeting. Abstract PII 136, p. 688.
- MIYATA, M. & TAKEMOTO, K. (1978). *Makromol. Chem.* **179**, 1167–1173.
- PAVEL, N. V., QUAGLIATA, C. & SCARCELLI, N. (1976). *Z. Kristallogr.* **144**, 64–75.
- SOBOTKA, H. (1934). *Chem. Rev.* **15**, 311–375.
- TANG, C. P. (1978). PhD Thesis, The Feinberg Graduate School, The Weizmann Institute of Science, Rehovot, Israel.